



Published in final edited form as:

Pain. 2008 September 15; 138(3): 641–656. doi:10.1016/j.pain.2008.02.021.

Brain dynamics for perception of tactile allodynia (touch-induced pain) in postherpetic neuralgia

P. Y. Geha¹, M. N. Baliki¹, X. Wang¹, R. N. Harden², J. A. Paice³, and A. V. Apkarian^{1,4}

¹*Department of Physiology, Northwestern University, Feinberg School of Medicine, 303 East Chicago Ave, Chicago IL, 60611. USA.*

²*Rehabilitation Institute of Chicago, Northwestern University, Feinberg School of Medicine, 303 East Chicago Ave, Chicago IL, 60611. USA.*

³*Department of Medicine, Northwestern University, Feinberg School of Medicine, 303 East Chicago Ave, Chicago IL, 60611. USA.*

⁴*Departments of Anesthesia, Surgery, and Lurie Cancer Center, Northwestern University, Feinberg School of Medicine, 303 East Chicago Ave, Chicago IL, 60611. USA.*

Abstract

Postherpetic neuralgia (PHN) is a debilitating chronic pain condition often accompanied by a sensation of pain when the affected region is touched (tactile allodynia). Here we identify brain regions involved in stimulus-induced touch-evoked pain (dynamical mechanical allodynia, DMA), compare brain activity between DMA and spontaneous pain (described earlier for the same patients in [28]), delineate regions that specifically code the magnitude of perceived allodynia, and show the transformation of allodynia-related information in the brain as a time-evolving network. Eleven PHN patients were studied for DMA and its modulation with Lidoderm therapy (patches of 5% lidocaine applied to the PHN affected body part). Continuous ratings of pain while the affected body part was brushed during fMRI were contrasted with non-painful touch when brushing was applied to an equivalent opposite body site, and with fluctuations of a bar observed during scanning, at three sessions relative to Lidoderm treatment. Lidoderm treatment did not decrease DMA ratings but did decrease spontaneous pain. Multiple brain areas showed preferential activity for allodynia. However, mainly responses in the bilateral putamen and left medial temporal gyrus were related to the magnitude of allodynia. Both DMA and spontaneous pain perceptions were best represented within the same sub-cortical structures but with minimal overlap, implying that PHN pain modulates behavioral learning and hedonics. These results have important clinical implications regarding adequate therapy.

Keywords

Chronic pain; fMRI; touch; putamen; amygdala; cortex

Correspondence should be addressed to A. Vania Apkarian, Department of Physiology, Northwestern University Medical School, 5-120 Ward Building, 303 E. Chicago Ave. Chicago IL, 60611. USA. E-mail: a-apkarian@northwestern.edu.

Publisher's Disclaimer: This is a PDF file of an unedited manuscript that has been accepted for publication. As a service to our customers we are providing this early version of the manuscript. The manuscript will undergo copyediting, typesetting, and review of the resulting proof before it is published in its final citable form. Please note that during the production process errors may be discovered which could affect the content, and all legal disclaimers that apply to the journal pertain.

There is no conflict of interest.

Introduction

Postherpetic neuralgia (PHN) is estimated to occur in 2–35% of subjects after reactivation of latent varicella-zoster virus [13,31,36–38]. It is characterized by the presence of pain of various qualities: 1) continuous burning or aching pain, 2) intermittent sharp pain, and 3) various sensory complaints, and is commonly accompanied by touch provoking a perception of pain (tactile allodynia, estimated incidence of 70–90%) [21–23,26,56]. Even though PHN often resolves with time, in some patients the pain persists for years, usually with a devastating impact on quality of life [18]. The condition is considered the prototypical human chronic neuropathic condition, because such patients exhibit multiple peripheral and central signs of neuropathy [49,50,63], yet there is very little information regarding the brain mechanisms involved in the condition, especially for tactile allodynia.

Allodynia has been studied for multiple clinical conditions [8,42,43,52,53,58,64], but not for PHN, as well as in healthy subjects following a mild skin injury [6,32,33,41,47,69]. These studies indicate that multiple brain regions demonstrate enhanced activity for allodynia. However, the actual relationship between brain activity and perceived allodynia has rarely been studied.

We recently described brain activity for spontaneous pain in PHN [28], where continuous ratings of spontaneous pain during fMRI were best correlated with activity in the basal ganglia and amygdala. Here we characterize brain activity in the same PHN patients when they continuously rate their tactile allodynia, assessed prior to and after 5% lidocaine patch treatment (a procedure that clinically reduces PHN pain [26,55]). We examine activity differences, regional activity correlations with magnitude of pain ratings, and the temporal relationship between brain activity and stimuli and ratings in order to specifically map properties of tactile allodynia with brain activity. Given our recent findings [5,28], our main hypothesis is that allodynia and spontaneous pain should be represented in similar brain regions, involving sub-cortical regions rather than cortical areas involved in the sensory representation of acute pain. On the other hand, we also hypothesize that brain activity for allodynia and spontaneous pain should show minimal overlap, mainly because animal studies [16,19,65], and human studies [43], indicate that distinct afferent fiber types and spinal cord processes mediate these perceptions.

Methods

Patients and screening procedures

Diagnostic criteria for recruitment and clinical and demographic characteristics of the patients were described in detail in our previous study, which was done on the same patients [28]. Briefly, patients were included if they fulfilled the IASP criteria for post-herpetic neuralgia (PHN). All the patients reported chronic spontaneous PHN pain (> 3 months) [36] with a pain magnitude of at least 3/10 on a visual analog scale (VAS). At the screening interview, patients were tested for dynamic mechanical allodynia (DMA) by passing a foam brush over the painful area. Presence of DMA was asserted if the patient reported an increase of the pain by at least 1 unit on the VAS.

Fourteen PHN patients were entered into the study. Only eleven were analyzed: nine females and two males, ranging in age from 46 to 85 (mean age 66.4), and spontaneous pain intensity on VAS ranged from 3 to 9 (mean 6.5) (see supplementary material for location of PHN on the body). One patient dropped out from the study, one did not complete all the sessions, and faulty registration of functional scans occurred for a third. One patient from the previous study did not complete all the sessions for this study, and was replaced by a new patient (male, 48 years old, with a lesion on the right side of the neck, spontaneous pain intensity of 9). The

Northwestern University Institutional Review Board approved this study, and written informed consent was obtained from all participants.

Experimental design and ratings

Patients were scanned under three different conditions using a semi-block design. During the scans we label *a*, they received a gentle brushing to the sensitive body area to elicit DMA; during scans we label *t*, they received a similar light-touch control stimulus on the non-painful mirror body side. Just before entering the scanner, the area showing DMA and the non-painful mirror body side were marked on the body. The marked regions were brushed manually using a foam brush that applies approximately 10 gm of force, at a rate of about 1 Hz to provoke DMA. Patients rated their total pain during both *a* and *t* scans. They performed another control scan *v* by rating the length of a moving bar approximating the variability of their DMA pain scan *a*. The *a* and *t* scans were repeated in random order (maximum three per session), and the *v* scan was always last (one per session).

Stimulation episodes were variable with a mean duration of 32 ± 14 s and a distribution shown in Fig. 1B. During a certain run, the length of each stimulus episode was varied to minimize anticipatory responses. Patients were asked to continuously rate their total pain during both tasks *a* and *t* using a finger-span logging device, while observing their ratings online, projected on a screen as a moving bar (bar size scaled from 0 to 10; 0 = no pain; 10 = worst imaginable pain) [2,5,24,28]. During the *a* scans, ratings represent fluctuations of the spontaneous PHN pain in episodes of no stimulation, and of both the spontaneous and DMA pain in episodes of stimulation; whereas during the *t* scans it represents the spontaneous pain only because, in this case, the stimulus was perceived as pure touch (subjects were specifically instructed not to rate non-painful touch perception, and none of the patients reported any touch-evoked pain from the control side). An example of pain rating during an *a* scan is shown in Fig. 1A. The *v* scans were done using the same finger-span logging device.

Our setup offers the advantage of studying brain components related to stimulation episodes (S_a , S_t , and S_v , vectors defining stimulus periods for DMA, touch, and visual lengths) and brain components related to rating various perceptions (R_a and R_v , vectors derived from rating periods). Patients were scanned during three different sessions to investigate the effect of treatment of the PHN condition with Lidoderm patches (topical 5% lidocaine) after acute and long-term use. Brain scan session 1 was done at baseline before the start of treatment, session 2 after six hours of use of the Lidoderm patch, and session 3 after two weeks of continuous use of the Lidoderm patch.

Functional magnetic resonance data acquisition

Functional MRI data was acquired with a 3T Siemens Trio whole-body scanner with echo-planar imaging (EPI) capability using the standard radio-frequency head coil. fMRI and anatomical MRI acquisition details are the same as in our previous study [28].

fMRI data analysis

Patients in pain invariably move in the scanner. To compensate for motion artifacts we performed a correction in two steps. The first step consisted in standard correction for head motion (FMRIB's Software Library, [60], www.fmrib.ox.ac.uk/fsl), which generated a time course for head motion. In the second step we included this time course as a variable of no interest in the general linear model design used to search for events of interest.

The following pre-processing was applied to the motion corrected data: slice-timing correction using Fourier-space time-series phase-shifting; non-brain removal using BET; spatial smoothing using a Gaussian kernel of FWHM 5 mm; global (volumetric) multiplicative mean

intensity renormalization; and registration to standard space using each subject's high-resolution anatomic images as an intermediate step.

Five of our subjects had their lesion on the right side. The orientation of the raw data (scan a) was flipped for those five subjects, so their activity was represented as if they had the lesion on the left side. The six subjects with a left sided lesion had their control scans (scan t) flipped to the left side. Therefore, all scans used for both tasks represented left sided stimulation. To test for differences between flipped and unflipped activity maps, we also examined brain activity for DMA where the analysis described below was done in the original orientation (see Supplementary Fig. 1).

Ratings from scans a and v respectively (Fig. 1A, black tracing), as well as stimuli from scans a and t , were binarized, convolved with a canonical hemodynamic response function, and used *separately* in a general linear model as primary vectors of interest (Sa , St , Ra , Rv). The model included two vectors, one for the event of interest and the other for the time course of head motion (as a covariate of no interest). A 200s high-pass temporal filter was used for all scans.

Identifying activity maps for DMA

Group averaged activity maps were determined using FILM with local autocorrelation correction [66]. Averaged activity maps were computed across subject and across treatment sessions [$(Sa)all$, $(Ra)all$, $(St)all$, and $(Sv)all$, group averaged activity for each task and vector]. To specifically isolate brain activity related to DMA, higher level contrasts were performed across all treatment sessions, in order to identify: 1) brain regions more active for DMA in contrast to touch, based on the timings of applied stimuli, i.e., $(Sa - St)all$; 2) brain regions more active for DMA in contrast to touch, based on the timings of ratings of perceived DMA, i.e., $(Ra - St)all$. To identify regions of overlap between the latter two maps we performed a conjunction analysis, where activity in one map is binarized and multiplied with the second map, performed in both directions. We also contrasted between maps determined for DMA based on stimulus timings and based on ratings of perceived pain (paired t-test), $\{(Sa - St) - (Ra - St)\}all$, (masked by activity for $(Sa)all > 0$ to avoid false positives) for all subjects and across treatment sessions.

All higher-level analyses were computed using age and pain durations as variables of no interest, which reduced the variability of the activations. As in the previous study, we observed an overall effect of spontaneous pain on brain activity independent from the task; we accordingly corrected for differences in spontaneous pain within each subject when computing $(Sa - St)all$ and $(Ra - St)all$ by adding spontaneous pain magnitude as a variable of no interest. Only positive activity was determined for these contrasts. All maps were specifically examined to insure the lack of false positive activity. Z-statistic images were thresholded at $z > 2.3$ and a (repeated-measures corrected) cluster significance threshold of $P = 0.01$ [67].

Comparing DMA to spontaneous pain

To determine brain activation similarities and differences between DMA and spontaneous pain, we calculated conjunction and contrast maps between these activation maps. We performed a paired t-test contrast between DMA scans and spontaneous pain (Rsp) scans (contrast for spontaneous pain ratings from visual bar length ratings, $Rsp - Rv$) using ten patients who had performed both tasks (see [28]). This contrast was first performed using a random effects analysis $\{(Sa-St)-(Rsp-Rv)\}all$ (masked with $(Sa-St)all > 0$ to avoid false positives). As the total pain magnitude was unmatched, we performed a second fixed effects contrast after including total pain as a covariate of *interest*, masked appropriately. The opposite contrast was similarly also performed.

Region of interest-based analysis—A region of interest (ROI) analysis was performed on each subject and each scan to relate regional brain activity to ratings of DMA pain and to examine the temporal properties of regional brain activity relative to stimulus and perception timings. The ROIs were defined from group averaged activity maps, masked by a macroscopic anatomical parcellation of the MNI MRI single-subject brain [61]. The ROIs were reverse-normalized and projected back into the un-normalized individual brain space. Subdivisions between the amygdala, extended amygdala, and hippocampus were performed using coordinates derived from [40]. Average z-scores and average fMRI BOLD activity were calculated over all voxels within each ROI, for each scan.

We compared average z-scores between *a* ($n = 51$ from 11 patients) and *t* ($n = 46$ from 11 patients) scans using an unpaired t-test at a significance level of $P < 0.01$. We also examined the relationship between DMA intensities, and z-scores using linear correlations. The average BOLD signal for the total trial for a given ROI was submitted to cross-correlation analysis with stimuli and ratings.

Isolating DMA magnitudes from ratings—In order to separate spontaneous pain from DMA -related pain ratings for each *a* scan, we calculated the average change in pain rating from baseline spontaneous pain, which we designate average- Δ pain for each scan. We tested treatment effects on average- Δ pain using one-way ANOVA.

Temporal properties of pain ratings and of regional brain activity—We examined the temporal response pattern for ratings of DMA and all activity extracted from ROIs, relative to the start and end of stimulation, within a fixed time window. Window width was based on the mode of stimulus duration (Fig. 1B). Stimulus timing-triggered average DMA ratings (time dependent Δ pain), total pain (spontaneous pain + DMA), or ROI fMRI BOLD responses were determined across subjects and sessions, and contrasted using 2-way repeat-measure ANOVA (factor 1 = treatment sessions or scan conditions; factor 2 = time which was the repeat measure of time steps in TR).

Cross-correlation analyses—The inter-relationships among ROI BOLD activity, stimuli, and DMA pain ratings were examined by calculating normalized linear cross-correlations among them, after convolving vectors *a*, *t*, and *v* with the hemodynamic response. The resultant time function indicates the extent of similarity (peak value which designates probability of similarity or dissimilarity; value range -1 to $+1$), the phase shift (peak lead or lag from time zero) between continuous stationary random variables, and the change in similarity at the various shifts examined. It is calculated by convolving the two random variables (i.e., (ROI BOLD)*(*a***h*), (ROI BOLD)*(*t***h*), (ROI BOLD)*(*v***h*), where *h* = hemodynamic response, * = cross-correlation or convolution). Cross-correlation at zero lag is the same as the linear correlation between the variables, and cross-correlation at a given time lag is also equivalent to the linear correlation when one of the appropriate variables is time shifted by the same lag. This method has been extensively used in electrophysiology to identify network connectivity properties between pairs of neurons [46]. Activations determined in fMRI studies, can be considered the outcome of cross-correlating the task vector with brain activity, at lag zero. Notably, there are no additional assumptions necessary for the application of cross-correlation to fMRI than those assumed for general linear modeling analyses.

In the present study, stimuli and ratings were digitized at the fMRI data acquisition rate. Given that the stimuli were variable in duration and the ratings variable in duration and intensity, the cross-correlation between regional BOLD and hemodynamic response-convolved stimuli and ratings provides an optimal measure for differentiating between brain regional functional properties. Cross-correlations were averaged across scans, and correlation coefficients and delays compared between regions and conditions.

DMA perception related brain networks

Correlational network maps were generated using the fMRI BOLD activity time course from a seed region, and correlation coefficients between it and the time course of all other brain voxels were computed, following the procedures of Fox et al. [25]. BOLD time courses were extracted from functional scans processed with slice time correction, motion correction using MCFLIRT, spatial smoothing using a Gaussian kernel of full-width-half-maximum 5 mm, nonlinear high-pass temporal filtering, and intensity normalization. The time course of average BOLD within the seed region was used, after different time delays or time advances, to determine all brain voxels correlated or anti-correlated to it. To combine results across subjects and compute statistical significance, correlations were transformed to z-scores, and maps generated using fixed-effects analysis corrected for multiple comparisons at a significance level $p < 0.01$. Only ten patients were included in this analysis, as one subject's average correlational map was noisy.

Results

Brushing the PHN site during fMRI scans resulted in increased ratings of pain (example shown in Fig. 1A) in all subjects. Moreover, brushing the equivalent contralateral body side did not change pain ratings, and the patients reported no touch-evoked pain sensations for this control stimulus.

Influence of lidocaine treatment on DMA

Treatment with the Lidoderm patch did not decrease DMA ratings but did decrease ratings of spontaneous pain. The change in pain ratings for touch stimuli applied to the PHN-affected zone was examined for average- Δ pain and time dependent Δ pain. Average- Δ pain across all patients was 1.8 ± 0.3 for session 1 (mean \pm SEM), 2.7 ± 0.6 for session 2, and 2 ± 0.4 for session 3 ($F_{2,48} = 0.89$, $P = 0.42$), and did not change with treatment. The time-dependent measure of DMA, Δ pain measured from either start or end of painful stimuli (Fig. 1D), also did not decrease with treatment. Instead it showed a slight increase after a six-hour lidocaine treatment ($F_{2,48} = 0.8$, $P = 0.45$ for epochs of increasing pain; $F_{2,48} = 1.5$, $P = 0.2$ for epochs of decreasing pain). Total pain (spontaneous pain + DMA pain), on the other hand, decreased significantly for epochs of increasing pain ($F_{2,48} = 3.5$, $P < 0.05$), and for epochs of decreasing pain ($F_{2,48} = 3.7$, $P < 0.05$) (Fig. 1C), due to the decrease in spontaneous pain with treatment.

Brain activity for DMA in PHN

To isolate brain activity for DMA in PHN, we examined contrasts between DMA provoking and touch inducing scans, in relation to stimulus timings and in relation to the ratings of DMA, across the three treatment sessions and after correcting for covariates of no interest for head motion, age, pain duration, and spontaneous pain. Areas showing more activity for DMA than touch as identified relative to stimulus timings (random effects, $(Sa - St)_{all}$) (Fig. 2A and Table 1; also Supplementary Fig. 2) included the cerebellum, brainstem (PAG, substantia nigra, red nucleus), right (contralateral to stimulation) thalamus, bilateral striatum, bilateral insula, left MT (visual motion perception area), right inferior frontal gyrus, supplementary motor cortex (SMA), anterior cingulate (ACC), left dorsal amygdala/extended amygdala (SLEA), and left medial temporal gyrus (MTG, including posterior SLEA and parts of the hippocampus). Therefore, compared to touch, we observe enhanced activity for DMA in cortical, sub-cortical, and brainstem regions. This result is consistent with earlier reports for DMA examined in patients with trigeminal neuropathy [8], patients with peripheral or central neuropathies [52, 53,64], and patients with complex regional pain syndrome [42].

Our experimental design is based on the notion that monitoring subjective ratings of DMA should provide more accurate information regarding the characteristics of the pain, and thus

we hypothesized that assessing DMA relative to its ratings should show greater and more specific brain activity. Testing for DMA relative to timings of ratings (random effects, $(Ra - St)_{all}$) shows significant clusters in the cerebellum and left MT, with weaker activity (sub-threshold clusters) in bilateral basal ganglia and insula. Thus, contrary to our expectation, the rating based DMA map was more restricted than the stimulus based map. To explore the relationship between these two representations, we examined their conjunction and contrast for a less stringent statistical threshold (fixed effects design).

There was complete overlap (100%) between the fixed effects map derived from the ratings and the equivalent map derived from stimulus timings, while only 31% of the activity derived from the stimulus timings overlapped with that derived from pain ratings (Fig. 2B; also Supplementary Figs 3 & 4). Given that more extensive activations were observed in the map derived from stimulus timings, this was tested statistically in a higher-level contrast (fixed effects, $\{(Sa - St) - (Ra - St)\}_{all}$). The result confirms the differences shown in the conjunction, indicating that the stimulus timing derived map was associated with significantly more activity, but only in cortical areas (Fig. 2C, and Table 2; also Supplementary Fig. 5). The spatial differences imply that regions overlapping between the two maps (sub-cortical areas) are better related to DMA. In the time domain, the two maps explore different phases of pain perception (see inset in Fig. 2C). From this perspective, activity differences are either due to greater activity in the early phase of stimulation (implying the presence of touch responses in the early phase) or to lower activity in the late phase of DMA when the perception of pain is decreasing. The opposite contrast did not yield any significant clusters.

Comparison between brain activations for spontaneous and DMA pain

To examine the spatial relationship between brain regions associated with DMA pain and spontaneous pain in PHN patients (the latter derived from [28]), we performed conjunction and contrast comparisons between the two tasks (random effects results). Overlaying the two maps on a single brain indicates that both conditions activate very similar areas. The conjunction analysis, however, shows little overlap, only 5%, localized mainly to bilateral insula (Fig. 3A). Contrasting the activations for spontaneous pain from DMA (random effect, $\{(Rsp - Rv) - (Sa - St)\}_{all}$) did not yield any significant clusters. On the other hand, the opposite contrast showed enhanced DMA related activity in the cerebellum, brainstem, right thalamus, bilateral putamen, bilateral insula, and right inferior frontal gyrus (not shown). We interpret this result as being a consequence of the fact that pain ratings during DMA are not matched to those during spontaneous pain.

On average, patients reported significantly more total pain during DMA (4.7 ± 0.4) than during spontaneous pain scans (3.6 ± 0.3) (t-test; $p < 0.05$). Therefore, we contrasted DMA and spontaneous pain after regressing with total pain to specifically identify brain regions that are related to total pain and are more active in each condition. Spontaneous pain activated significantly more right caudate and ventral striatum and bilateral insula (Fig. 3B, Supplementary Table 4 and Figs. 7 & 8), while DMA activated significantly more right (contralateral to PHN) SII, insula, dorsal amygdala, and bilateral putamen and globus pallidus; additionally, areas corresponding to the rating task were activated more for DMA including left SMA, MI, pre-motor, and SI (hand representation in the hemisphere contralateral to the fingers used in ratings even though some of these brain were flipped changing sidedness for the ratings); visual motion areas were also activated more in DMA. The fact that during DMA the ratings are more robust and more frequent readily explains observed task related sensorimotor and visual differences. There was segregation within the basal ganglia with spontaneous pain mapping to the caudate and ventral striatum, while DMA mapping to the putamen and globus pallidus bilaterally. Moreover, within the anterior insula/IFG region, DMA was preferentially localized to the right (contralateral to PHN), while spontaneous pain was

localized to the left. Thus, we observe specific regional representational differences between DMA and spontaneous pain, which became apparent only after correcting for pain magnitudes.

Regional analysis

To segregate brain regional responses with regard to their specific relationship to DMA, we examined response size (average z-scores) and temporal properties of the fMRI BOLD signal, and related them to stimulus timings and perception ratings. The specific regions examined were based on the contrasts of DMA with touch and with spontaneous pain. We examined all twelve regions identified at the random effects comparisons (except SII, which was identified from fixed effects contrast between DMA and spontaneous pain): ACC, SMA, right thalamus, right SII, left amygdala/SLEA, left MTG, and left and right basal ganglia, insula, and frontal cortex. Three brain regions showed best specificity for DMA: left and right putamen, and left MTG. In all three areas: 1) mean activity was significantly larger for DMA in contrast to non-painful touch, or in contrast to visual bar length ratings, and did not significantly change with treatment (Fig. 4 bar graphs); 2) activity was positively correlated with magnitude of DMA ratings (these correlations were mostly preserved when data was segregated for each treatment session; data not shown), but was not related to visual bar length ratings (Fig. 4 scatter plots); 3) stimulus-triggered averaged fMRI responses and cross-correlations of fMRI BOLD with either the stimuli or ratings of DMA were significantly larger than equivalent measures for touch or visual rating tasks (Fig. 5, Table 3 and Supplementary Table 3).

Details of the time course of BOLD responses (stimulus start and end triggered average regional BOLD, and the cross-correlations of regional BOLD with the stimuli or ratings, convolved with hemodynamic response function) provide important insights and need further description. The cross-correlational analysis measures brain activity in relation to stimuli and ratings by accounting for the complete time course of the fMRI signal, thus providing a normalized metric of similarity between brain activity, stimuli, and ratings over the whole time course of the task and also identifies temporal shifts in relation to stimuli and ratings.

Relative to the application of DMA-inducing stimuli and their predicted response (convolved with hemodynamic response), stimulus-triggered group-averaged pain ratings were delayed and continued to increase within the time window examined. Relative to the end of stimulation, however, the ratings were sustained and only slowly returned to baseline, resulting in an overall averaged cross-correlation where the peak is delayed by at least 7.5 s between stimulus and rating of DMA. (This time delay is larger than the raw time delay observed, and is the result of the low pass filtering imposed by the convolution with the hemodynamic function (compare Fig. 1D to Fig. 5A), but the convolution imposes the same assumptions as those for the fMRI signal and enables direct comparisons among fMRI and stimuli and ratings.) In contrast, for the visual length-rating task the increasing and decreasing phases of the ratings were more similar to the predicted responses, and resulted in a stimulus-response cross-correlation that is symmetric around time zero (Fig. 5B). At the start of DMA-inducing stimulation, average stimulus-triggered BOLD responses in left and right putamen and left MTG (Fig. 5C and 5D) increased rapidly, matching more closely to the time course of the stimulus than the ratings, and were sustained within the time window examined. All three regions also responded to touch but to a lesser extent. In the time window around the end of DMA-inducing stimulation, BOLD responses in all three regions were not different between DMA and touch (Table 3). BOLD responses in all three areas to non-painful touch and to visual bar length ratings were smaller, transient, or not present. Cross-correlations between activity and stimuli or ratings show that the BOLD signal in all three areas was better correlated with the DMA task than with non-painful touch or with visual bar length ratings.

Given the time delay between the stimulus and rating of DMA, the temporal relationship of brain activity is informative and is best identified from cross-correlation results. Cross-

correlations during DMA for left and right putamen indicate that their activity was delayed by about 2.5–5 s (1–2 TRs) from the start of the stimulus, and led perception of DMA by another 2.5–5 s. The left MTG response also showed similar, but smaller, time differences between stimulus and ratings. Thus, even though the activity in each of these three regions shows the best properties for coding DMA, in each case it preceded the perception of DMA by only a few seconds (a few TRs), and in no case showed a better correlation with DMA at any of the time delays examined. Therefore, we conclude that while activity in these regions may be causally related to the perception of DMA, the regions themselves cannot be considered the sites where DMA is perceived.

Similar analyses and results for the ACC, right insula, right SII, and right thalamus ROIs are shown in Fig. 6. While the activity in the ACC, right insula, and thalamus (but not in the right SII) was significantly greater during DMA than during light touch, in no case was it correlated to the magnitude of DMA (average- Δ pain). Stimulus-triggered response in the ACC showed that this region has a robust response during DMA and does not respond to touch. Thus, the ACC is the region that best differentiates between DMA and touch. However, its activity was transient and its cross-correlation was best with the stimulus and preceded the stimulus (the cross-correlation peak was 2.5 s, 1 TR, earlier than the stimulus -- the fastest response seen of all areas studied). In addition, DMA ratings lagged behind ACC activity by more than 10 s. Right insula, , and right thalamus BOLD responses were generally similar for DMA and for touch, SII average brain activity and stimulus-triggered responses were robust and similar for both DMA and non-painful touch. This provides evidence that SII does not seem important in DMA, and that our control task evoked adequate brain responses. We further explored the relationship between DMA and brain activity by performing a whole-brain covariate analysis (Supplementary Fig. 9). The only new noteworthy region was an area in mid left insula, contiguous with MTG cluster. Regional analysis of this area indicated a borderline correlation with DMA (at coordinates: $-38, 4, -8$, with $r = 0.32$, and $p = 0.02$), after correcting for age and session.

Perception of DMA at brain network level

Given that the above analyses do not show any brain region where activity best relates to DMA, especially regarding temporal evolution relative to perception of DMA, we sought to differentiate brain activity for this percept at the brain network level. Of the three areas showing specificity for DMA, the left putamen exhibited the best characteristics. Therefore, we searched for the network of brain activity related to this region. As the cross-correlation analysis indicated that left putamen activity, when advanced by 5 s (2 TRs), relates best to the stimulus, while, when delayed by 5 seconds, it relates better with ratings of DMA, we determined brain connectivity when activity within this region was used as a seed at both time delays. Connectivity of left putamen seed at the time best related to the stimulus (-5 s, Fig. 7 left panel, Supplementary Table 5 and Supplementary Fig. 10) showed positive correlations mainly with sub-cortical structures (thalamus, basal ganglia, brainstem, cerebellum), in addition to the anterior insula/inferior frontal gyrus and orbitofrontal and inferior temporal cortex. Anticorrelated connectivity was observed mainly with the amygdala and posterior parietal cortex, as well as parts of the cingulate cortex and SMA. On the other hand, connectivity of left putamen seed at the time better related to perception of DMA ($+5$ s, Fig. 7 right panel, Supplementary Table 5 and Supplementary Fig. 11) showed positive correlations within the basal ganglia, bilateral thalamus and amygdala. In the cortex it was positively correlated with bilateral SI, parts of the insula, and posterior parietal regions, as well as cingulate and visual cortices and cerebellum. Anticorrelated connectivity was observed primarily with bilateral medial and orbital prefrontal cortex, smaller regions within precuneus and posterior cingulate, parts of the insula and parahippocampal gyrus, and inferior temporal cortex. Thus, the largest change in connectivity between the two time windows was for the parietal cortex, where

connections switched from negative to positive with the advancement of time, and in medial and orbital PFC, where in time connectivity became negative (see Supplementary Fig. 11, Supplementary Table 5). When connectivity was examined for left putamen seed with no time delays, the resultant network pattern was intermediate between the two described above. We also examined left putamen connectivity when its time signal was further advanced by +15 s (+6 TRs); no significant positive or negative correlations could be detected at this time delay. Overall, these results show the dynamics of brain connectivity as the DMA-related information engages various brain structures in opposing patterns. We observe that the positively correlated flow of information is initially limited mostly to a subcortical-brainstem network and that in time it then engages the cortex.

Discussion

This is the first demonstration of DMA pain-related brain activity in PHN and the first determination of the brain interrelationship between DMA and spontaneous pain in chronic pain. DMA, in contrast to non-painful touch, preferentially activated: 1) cortical areas thought to be involved in sensory (SII, insula), motor (MI, SMA, cerebellum), cognitive/working memory (PFC), and affective/attentional (ACC) processes; and 2) sub-cortical areas involved in sensory (thalamus), sensorimotor behavior (basal ganglia), and hedonics (MTG) processes. Most of these areas are seen to be activated by acute pain in normal subjects [1] and are also observed to be participating in DMA. Only a limited subset correlated significantly with the perceived magnitude of DMA, and none showed a better correlation to ratings of DMA in contrast to the stimulus provoking DMA. The latter prompted the search for a signature for DMA at the brain network level, where we could show a dramatic shift in brain connectivity as the stimulus is transformed to a perception of DMA.

In majority of earlier studies, a contrast was made between tactile allodynia and touch, and the identified regions were ascribed as being part of the brain network involved in the percept. Still, the contrast maps generated share many similarities to the map we report here. Our results differ from earlier studies in that mainly sub-cortical regions correlated with DMA magnitudes in PHN patients. Two prior studies tested the relationship between brain activity and magnitude of tactile allodynia. In one study [58] allodynia magnitudes were determined at the termination of brain scans, and these magnitudes correlated with anterior insular activity (after correcting for spontaneous pain). The second study had a design more similar to ours, where patients with chronic pain performed online ratings of touch-evoked allodynia [42], and the covariate analysis indicated that multiple cortical areas were positively correlated with allodynia ratings. They did not, however, correct for the presence and magnitude of spontaneous pain, or for patients' age or pain duration, and both studies did not perform ROI-based analysis. Given the differences in analysis among all three studies, it is not clear if the disparate results are due to the distinct patient populations or to the different methods used.

Caveats

The current study, like most brain imaging studies of chronic pain [1], suffers from the limited number of patients included. We compensated for this by performing repeat scans at different time points relative to lidocaine treatment. Another weakness regards differences in the body regions where PHN pain was present, partially compensated for by inverting the brain to render the stimulus and PHN pain always on the left side. Lack of a placebo arm and the method of rating used also complicate interpretation of the results (discussed further below).

Lidoderm treatment effects on PHN pain

Participants were instructed to rate their overall pain. We chose this approach as the interaction between spontaneous pain and DMA is unknown, and also because spontaneous pain fluctuates

unpredictably [24]. We were surprised by the fact that the magnitude of DMA was not modulated by lidocaine therapy (based on a large number of events; $n = 295$), even though spontaneous pain did decrease with this treatment, as clinical trials indicate similar decreases in both when PHN patients are treated with Lidoderm [26,27,45,62]. It is possible that the differential efficacy was related to our method of rating pain (instantaneous ratings, while clinical studies are based on questionnaires which rely on the past memory of the patient). On the other hand, this result is consistent with the idea that DMA and spontaneous pain may underlie distinct processes, validated by the demonstration of minimal representational overlap between activations for each. These results also suggest that lidocaine may differentially interfere with excitability of afferents involved in spontaneous pain, whereas DMA may be more of a central phenomenon which topical drugs cannot affect [16,19]. Given that the current study did not have a placebo arm, we cannot discount the possibility that differential effects of lidocaine may be due to spontaneous pain being more susceptible to suggestion.

Brain activity differences between acute pain and DMA in PHN

When we examined brain activity in response to thermal painful stimuli in healthy subjects or in CBP, using the same methods as in the present study (with comparable numbers of subjects and stimuli), we observed that multiple cortical regions robustly code the perceived magnitude of pain [3,4]. Thus, the brain regions involved in DMA in PHN seem different from those associated with thermal pain perception. On the other hand, brain regions showing best specificity for thermal pain were mainly localized to the basal ganglia and thalamus in the normal subjects [4], while for PHN DMA the most specific responses were localized to the basal ganglia and MTG. The latter suggests that DMA in PHN is preferentially mediated through spinal-basal ganglia [14], spinal-parabrachial-amygdala [9], and spinal-amygdala [15] projections.

Role of basal ganglia and MTG in PHN pain

A recent study indicates differential involvement of various sub-portions of basal ganglia in pain, with the caudate and putamen reflecting sensory and emotional components of pain and the ventral striatum being associated with negative affect and fear [59]. Consistent with this, others show that dopamine receptor binding in the putamen is correlated with heat pain thresholds [44,51]; that painful stimuli activate the putamen somatotopically [10]; putamen responds to tonic painful stimulation but not to nonpainful stimulation [20]; an acute infarct limited to the putamen can give rise to deep pain [57]; and nociceptive neurons are described in the region [17]. There has been little information regarding the role of basal ganglia in chronic pain conditions, but it is implicated in atypical facial pain and in burning mouth syndrome [30,35] and in tactile allodynia in trigeminal neuropathy [8]. Our results show involvement of the region in CBP spontaneous pain and in PHN for spontaneous pain and DMA. Spontaneous pain seems to involve the limbic portion (ventral striatum), while DMA involves the sensorimotor portion (putamen), suggesting that the former affects motivated behavior while the latter affects habitual behavior and sensorimotor processing [68].

We observe activation of the dorsal amygdala/SLEA as well as a more posterior MTG region. Only the latter was related to perceived DMA. The activated region of MTG includes posterior SLEA, and there is good evidence that the amygdala/SLEA is involved in pain. Multiple studies show that it is activated with acute and tonic pain [7,11,12,39,70,71], and animal studies indicate sensitization of amygdala responses to noxious stimuli in inflammatory and neuropathic models [34,48]. Therefore, the current results suggest that DMA also modulates hedonics, as does spontaneous pain in the CBP and in PHN.

Temporal evolution of DMA as a brain network

Continuous rating of perceived pain allowed studying the temporal properties of brain activity. The results indicate that the ACC shows the earliest response, with the latest responses seen in DMA-specific regions (putamen). However, even the most specific responses, on average, were better correlated to the stimulus and preceded the pain ratings, implying that the perception is due to the interaction of the activity at these sites with the rest of the brain. Consistent with this notion is our demonstration that at a time when putamen activity is best related to the stimulus, the parietal cortex is negatively engaged with this information; while when putamen activity is best related to DMA, many parietal areas reflect this information. The latter network shares many components with the brain default mode network [25,29,54] proposed to provide the balance of opposing forces with which incoming information may be interpreted. As correlations are transitive, and given that putamen activity was correlated to perceived magnitude of DMA, we can state that the networks identified are also correlated to the magnitude of DMA and, as such, the observed spatio-temporal change in brain connectivity reflects transmission of DMA information within the brain.

Conclusions

Overall, these results indicate that, on the one hand, in PHN patients both spontaneous pain and DMA engage sub-cortical regions involved in motivation, sensorimotor behavior, and hedonics, and impinge on separate portions of the basal ganglia, thus, distinctly impacting on various types of learned behavior. On the other hand, perception of DMA might be better characterized at the brain network level, where spatio-temporal dynamics of information flow across the network may be more informative.

Supplementary Material

Refer to Web version on PubMed Central for supplementary material.

Acknowledgements

We thank all the patients who participated in this study. We thank Dr. D. R. Chialvo for his advice, suggestions on data analysis, and comments on the manuscript. We also thank Drs. S. Khan, M. Martina, V. Szoros, and P. Montoya for their comments on earlier versions of the manuscript, and S. Apkarian for her help in editing the language. Supported by NIH grant R01 NS 35115 from the National Institute of Neurological Diseases, and by a grant from Endo Pharmaceuticals. Endo Pharmaceuticals also supplied the Lidoderm patches for this study, but had no role in its execution, the interpretation of the results, or writing or revising this manuscript.

Reference List

1. Apkarian AV, Bushnell MC, Treede RD, Zubieta JK. Human brain mechanisms of pain perception and regulation in health and disease. *Eur J Pain* 2005;9:463–484. [PubMed: 15979027]
2. Apkarian AV, Krauss BR, Fredrickson BE, Szeverenyi NM. Imaging the pain of low back pain: functional magnetic resonance imaging in combination with monitoring subjective pain perception allows the study of clinical pain states. *Neurosci Lett* 2001;299:57–60. [PubMed: 11166937]
3. Baliki M, Apkarian AV. The neurological effects of chronic pain. *PainEurope* 2006;4–5.
4. Baliki M, Geha PY, Chialvo DR, Apkarian AV. So what brain areas are specific for pain perception. *Neurosci Abstr* 2006:445.
5. Baliki MN, Chialvo DR, Geha PY, Levy RM, Harden RN, Parrish TB, Apkarian AV. Chronic pain and the emotional brain: specific brain activity associated with spontaneous fluctuations of intensity of chronic back pain. *J Neurosci* 2006;26:12165–12173. [PubMed: 17122041]
6. Baron R, Baron Y, Disbrow E, Roberts TP. Brain processing of capsaicin-induced secondary hyperalgesia: a functional MRI study. *Neurology* 1999;53:548–557. [PubMed: 10449119]
7. Becerra L, Breiter HC, Wise R, Gonzalez RG, Borsook D. Reward circuitry activation by noxious thermal stimuli. *Neuron* 2001;32:927–946. [PubMed: 11738036]

8. Becerra L, Morris S, Bazes S, Gostic R, Sherman S, Gostic J, Pendse G, Moulton E, Scrivani S, Keith D, Chizh B, Borsook D. Trigeminal neuropathic pain alters responses in CNS circuits to mechanical (brush) and thermal (cold and heat) stimuli. *J Neurosci* 2006;26:10646–10657. [PubMed: 17050704]
9. Bernard JF, Bester H, Besson JM. Involvement of the spino-parabrachio - amygdaloid and - hypothalamic pathways in the autonomic and affective emotional aspects of pain. *Prog Brain Res* 1996;107:243–255. [PubMed: 8782523]
10. Bingel U, Glascher J, Weiller C, Buchel C. Somatotopic representation of nociceptive information in the putamen: an event-related fMRI study. *Cereb Cortex* 2004;14:1340–1345. [PubMed: 15217895]
11. Bingel U, Quante M, Knab R, Bromm B, Weiller C, Buchel C. Subcortical structures involved in pain processing: evidence from single-trial fMRI. *Pain* 2002;99:313–321. [PubMed: 12237210]
12. Bornhovd K, Quante M, Glauche V, Bromm B, Weiller C, Buchel C. Painful stimuli evoke different stimulus-response functions in the amygdala, prefrontal, insula and somatosensory cortex: a single-trial fMRI study. *Brain* 2002;125:1326–1336. [PubMed: 12023321]
13. Bowsher D. The lifetime occurrence of Herpes zoster and prevalence of post-herpetic neuralgia: A retrospective survey in an elderly population. *Eur J Pain* 1999;3:335–342. [PubMed: 10700361]
14. Braz JM, Nassar MA, Wood JN, Basbaum AI. Parallel "pain" pathways arise from subpopulations of primary afferent nociceptor. *Neuron* 2005;47:787–793. [PubMed: 16157274]
15. Burstein R, Potrebic S. Retrograde labeling of neurons in the spinal cord that project directly to the amygdala or the orbital cortex in the rat. *J Comp Neurol* 1993;335:469–485. [PubMed: 8227531]
16. Campbell JN, Meyer RA. Mechanisms of neuropathic pain. *Neuron* 2006;52:77–92. [PubMed: 17015228]
17. Chudler EH. Response properties of neurons in the caudate-putamen and globus pallidus to noxious and non-noxious thermal stimulation in anesthetized rats. *Brain Res* 1998;812:283–288. [PubMed: 9813370]
18. Davies L, Cossins L, Bowsher D, Drummond M. The cost of treatment for post-herpetic neuralgia in the UK. *Pharmacoeconomics* 1994;6:142–148. [PubMed: 10147439]
19. Devor M. Sodium channels and mechanisms of neuropathic pain. *J Pain* 2006;7:S3–S12. [PubMed: 16426998]
20. Downar J, Mikulis DJ, Davis KD. Neural correlates of the prolonged salience of painful stimulation. *Neuroimage* 2003;20:1540–1551. [PubMed: 14642466]
21. Dworkin RH. An overview of neuropathic pain: syndromes, symptoms, signs, and several mechanisms. *Clin J Pain* 2002;18:343–349. [PubMed: 12441827]
22. Dworkin RH, Portenoy RK. Pain and its persistence in herpes zoster. *Pain* 1996;67:241–251. [PubMed: 8951917]
23. Fields HL, Rowbotham M, Baron R. Postherpetic neuralgia: irritable nociceptors and deafferentation. *Neurobiol Dis* 1998;5:209–227. [PubMed: 9848092]
24. Foss JM, Apkarian AV, Chialvo DR. Dynamics of pain: fractal dimension of temporal variability of spontaneous pain differentiates between pain States. *J Neurophysiol* 2006;95:730–736. [PubMed: 16282201]
25. Fox MD, Snyder AZ, Vincent JL, Corbetta M, Van Essen DC, Raichle ME. The human brain is intrinsically organized into dynamic, anticorrelated functional networks. *Proc Natl Acad Sci U S A* 2005;102:9673–9678. [PubMed: 15976020]
26. Galer BS, Jensen MP, Ma T, Davies PS, Rowbotham MC. The lidocaine patch 5% effectively treats all neuropathic pain qualities: results of a randomized, double-blind, vehicle-controlled, 3-week efficacy study with use of the neuropathic pain scale. *Clin J Pain* 2002;18:297–301. [PubMed: 12218500]
27. Galer BS, Rowbotham MC, Perander J, Friedman E. Topical lidocaine patch relieves postherpetic neuralgia more effectively than a vehicle topical patch: results of an enriched enrollment study. *Pain* 1999;80:533–538. [PubMed: 10342414]
28. Geha PY, Baliki MN, Chialvo DR, Harden RN, Paice JA, Apkarian AV. Brain activity for spontaneous pain of postherpetic neuralgia and its modulation by lidocaine patch therapy. *Pain* 2007;128:88–100. [PubMed: 17067740]

29. Greicius MD, Krasnow B, Reiss AL, Menon V. Functional connectivity in the resting brain: a network analysis of the default mode hypothesis. *Proc Natl Acad Sci U S A* 2003;100:253–258. [PubMed: 12506194]
30. Hagelberg N, Forssell H, Aalto S, Rinne JO, Scheinin H, Taiminen T, Nagren K, Eskola O, Jaaskelainen SK. Altered dopamine D2 receptor binding in atypical facial pain. *Pain* 2003;106:43–48. [PubMed: 14581109]
31. Helgason S, Petursson G, Gudmundsson S, Sigurdsson JA. Prevalence of postherpetic neuralgia after a first episode of herpes zoster: prospective study with long term follow up. *BMJ* 2000;321:794–796. [PubMed: 11009518]
32. Iadarola MJ, Berman KF, Zeffiro TA, Byas-Smith MG, Gracely RH, Max MB, Bennett GJ. Neural activation during acute capsaicin-evoked pain and allodynia assessed with PET. *Brain* 1998;121(Pt 5):931–947. [PubMed: 9619195]
33. Iannetti GD, Zambreau L, Wise RG, Buchanan TJ, Huggins JP, Smart TS, Vennart W, Tracey I. Pharmacological modulation of pain-related brain activity during normal and central sensitization states in humans. *Proc Natl Acad Sci U S A* 2005;102:18195–18200. [PubMed: 16330766]
34. Ikeda R, Takahashi Y, Inoue K, Kato F. NMDA receptor-independent synaptic plasticity in the central amygdala in the rat model of neuropathic pain. *Pain* 2007;127:161–172. [PubMed: 17055162]
35. Jaaskelainen SK, Rinne JO, Forssell H, Tenovu O, Kaasinen V, Sonninen P, Bergman J. Role of the dopaminergic system in chronic pain -- a fluorodopa-PET study. *Pain* 2001;90:257–260. [PubMed: 11207397]
36. Jung BF, Johnson RW, Griffin DR, Dworkin RH. Risk factors for postherpetic neuralgia in patients with herpes zoster. *Neurology* 2004;62:1545–1551. [PubMed: 15136679]
37. Katz J, McDermott MP, Cooper EM, Walther RR, Sweeney EW, Dworkin RH. Psychosocial risk factors for postherpetic neuralgia: a prospective study of patients with herpes zoster. *J Pain* 2005;6:782–790. [PubMed: 16326366]
38. Kost RG, Straus SE. Postherpetic neuralgia--pathogenesis, treatment, and prevention. *N Engl J Med* 1996;335:32–42. [PubMed: 8637540]
39. Kulkarni B, Bentley DE, Elliott R, Youell P, Watson A, Derbyshire SW, Frackowiak RS, Friston KJ, Jones AK. Attention to pain localization and unpleasantness discriminates the functions of the medial and lateral pain systems. *Eur J Neurosci* 2005;21:3133–3142. [PubMed: 15978022]
40. Mai, JK.; Assheuer, J.; Paxinos, G. Atlas of the human brain. San Diego: Academic Press; 1997.
41. Maihofner C, Handwerker HO. Differential coding of hyperalgesia in the human brain: a functional MRI study. *Neuroimage* 2005;28:996–1006. [PubMed: 16112876]
42. Maihofner C, Handwerker HO, Birklein F. Functional imaging of allodynia in complex regional pain syndrome. *Neurology* 2006;66:711–717. [PubMed: 16534108]
43. Maihofner C, Neundorfer B, Stefan H, Handwerker HO. Cortical processing of brush-evoked allodynia. *Neuroreport* 2003;14:785–789. [PubMed: 12858033]
44. Martikainen IK, Hagelberg N, Mansikka H, Hietala J, Nagren K, Scheinin H, Pertovaara A. Association of striatal dopamine D2/D3 receptor binding potential with pain but not tactile sensitivity or placebo analgesia. *Neurosci Lett* 2005;376:149–153. [PubMed: 15721212]
45. Meier T, Wasner G, Faust M, Kuntzer T, Ochsner F, Hueppe M, Bogousslavsky J, Baron R. Efficacy of lidocaine patch 5% in the treatment of focal peripheral neuropathic pain syndromes: a randomized, double-blind, placebo-controlled study. *Pain* 2003;106:151–158. [PubMed: 14581122]
46. Moore GP, Segundo JP, Perkel DH, Levitan H. Statistical signs of synaptic interaction in neurons. *Biophys J* 1970;10:876–900. [PubMed: 4322240]
47. Moulton EA, Pendse G, Morris S, Strassman A, Aiello-Lammens M, Becerra L, Borsook D. Capsaicin-induced thermal hyperalgesia and sensitization in the human trigeminal nociceptive pathway: an fMRI study. *Neuroimage* 2007;35:1586–1600. [PubMed: 17407825]
48. Neugebauer V, Li W, Bird GC, Bhave G, Gereau RW. Synaptic plasticity in the amygdala in a model of arthritic pain: differential roles of metabotropic glutamate receptors 1 and 5. *J Neurosci* 2003;23:52–63. [PubMed: 12514201]
49. Nurmikko T, Wells C, Bowsher D. Pain and allodynia in postherpetic neuralgia: role of somatic and sympathetic nervous systems. *Acta Neurol Scand* 1991;84:146–152. [PubMed: 1950450]

50. Oaklander AL. The density of remaining nerve endings in human skin with and without postherpetic neuralgia after shingles. *Pain* 2001;92:139–145. [PubMed: 11323135]
51. Pertovaara A, Martikainen IK, Hagelberg N, Mansikka H, Nagren K, Hietala J, Scheinin H. Striatal dopamine D2/D3 receptor availability correlates with individual response characteristics to pain. *Eur J Neurosci* 2004;20:1587–1592. [PubMed: 15355325]
52. Peyron R, Garcia-Larrea L, Gregoire MC, Convers P, Lavenne F, Veyre L, Froment JC, Manguiere F, Michel D, Laurent B. Allodynia after lateral-medullary (Wallenberg) infarct. A PET study. *Brain* 1998;121(Pt 2):345–356. [PubMed: 9549510]
53. Peyron R, Schneider F, Faillenot I, Convers P, Barral FG, Garcia-Larrea L, Laurent B. An fMRI study of cortical representation of mechanical allodynia in patients with neuropathic pain. *Neurology* 2004;63:1838–1846. [PubMed: 15557499]
54. Raichle ME. Neuroscience. The brain's dark energy. *Science* 2006;314:1249–1250. [PubMed: 17124311]
55. Rowbotham MC, Davies PS, Verkempinck C, Galer BS. Lidocaine patch: double-blind controlled study of a new treatment method for post-herpetic neuralgia. *Pain* 1996;65:39–44. [PubMed: 8826488]
56. Rowbotham MC, Fields HL. The relationship of pain, allodynia and thermal sensation in post-herpetic neuralgia. *Brain* 1996;119(Pt 2):347–354. [PubMed: 8800931]
57. Russmann H, Vingerhoets F, Ghika J, Maeder P, Bogousslavsky J. Acute infarction limited to the lenticular nucleus: clinical, etiologic, and topographic features. *Arch Neurol* 2003;60:351–355. [PubMed: 12633146]
58. Schweinhardt P, Glynn C, Brooks J, McQuay H, Jack T, Chessell I, Bountra C, Tracey I. An fMRI study of cerebral processing of brush-evoked allodynia in neuropathic pain patients. *Neuroimage* 2006;32:256–265. [PubMed: 16679031]
59. Scott DJ, Heitzeg MM, Koeppe RA, Stohler CS, Zubieta JK. Variations in the human pain stress experience mediated by ventral and dorsal basal ganglia dopamine activity. *J Neurosci* 2006;26:10789–10795. [PubMed: 17050717]
60. Smith SM, Jenkinson M, Woolrich MW, Beckmann CF, Behrens TE, Johansen-Berg H, Bannister P, De Luca CJ, Drobnjak I, Flitney DE, Nianzy R, Saunders J, Vickers J, Zhang Y, De Stefano N, Brady JM, Mathews PM. Advances in functional and structural MR image analysis and implementation as FSL. *Neuroimage* 2004;23(S1):208–219.
61. Tzourio-Mazoyer N, Landeau B, Papathanassiou D, Crivello F, Etard O, Delcroix N, Mazoyer B, Joliot M. Automated anatomical labeling of activations in SPM using a macroscopic anatomical parcellation of the MNI MRI single-subject brain. *Neuroimage* 2002;15:273–289. [PubMed: 11771995]
62. Wasner G, Kleinert A, Binder A, Schattschneider J, Baron R. Postherpetic neuralgia: topical lidocaine is effective in nociceptor-deprived skin. *J Neurol* 2005;252:677–686. [PubMed: 15778907]
63. Watson CP, Morshead C, Van der KD, Deck J, Evans RJ. Post-herpetic neuralgia: post-mortem analysis of a case. *Pain* 1988;34:129–138. [PubMed: 3174152]
64. Witting N, Kupers RC, Svensson P, Jensen TS. A PET activation study of brush-evoked allodynia in patients with nerve injury pain. *Pain* 2006;120:145–154. [PubMed: 16368192]
65. Woolf CJ, Salter MW. Neuronal plasticity: increasing the gain in pain. *Science* 2000;288:1765–1769. [PubMed: 10846153]
66. Woolrich MW, Behrens TE, Beckmann CF, Jenkinson M, Smith SM. Multilevel linear modelling for FMRI group analysis using Bayesian inference. *Neuroimage* 2004;21:1732–1747. [PubMed: 15050594]
67. Worsley KJ, Evans AC, Marrett S, Neelin P. A three-dimensional statistical analysis for CBF activation studies in human brain. *J Cereb Blood Flow Metab* 1992;12:900–918. [PubMed: 1400644]
68. Yin HH, Knowlton BJ. The role of the basal ganglia in habit formation. *Nat Rev Neurosci* 2006;7:464–476. [PubMed: 16715055]
69. Zambreau L, Wise RG, Brooks JC, Iannetti GD, Tracey I. A role for the brainstem in central sensitisation in humans. Evidence from functional magnetic resonance imaging. *Pain* 2005;114:397–407. [PubMed: 15777865]

70. Zubieta JK, Bueller JA, Jackson LR, Scott DJ, Xu Y, Koeppe RA, Nichols TE, Stohler CS. Placebo effects mediated by endogenous opioid activity on mu-opioid receptors. *J Neurosci* 2005;25:7754–7762. [PubMed: 16120776]
71. Zubieta JK, Smith YR, Bueller JA, Xu Y, Kilbourn MR, Jewett DM, Meyer CR, Koeppe RA, Stohler CS. Regional mu opioid receptor regulation of sensory and affective dimensions of pain. *Science* 2001;293:311–315. [PubMed: 11452128]

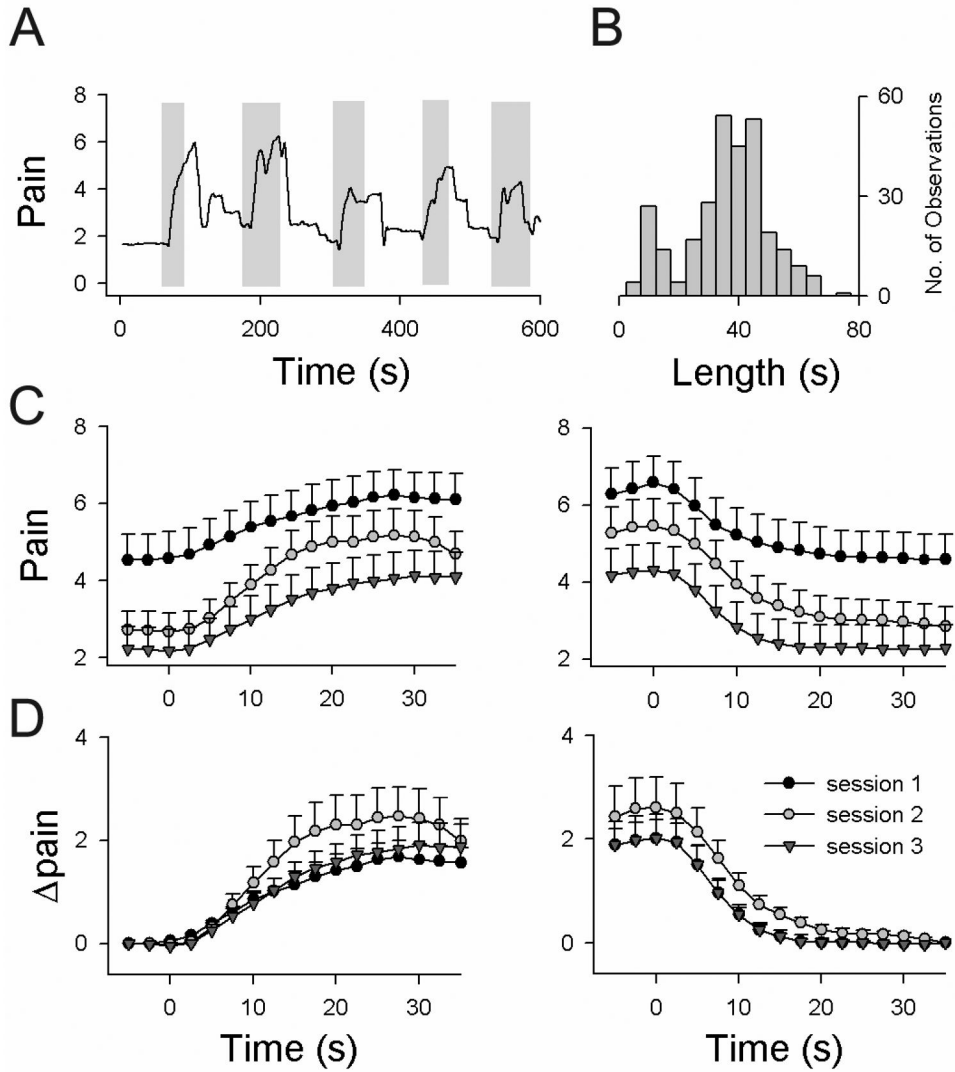


Figure 1. Treatment with topical lidocaine does not decrease DMA pain ratings
(A) Example of rating of DMA pain in one patient. Shaded rectangles delimit times when a stimulus was applied to the PHN body part. **(B)** Distribution of the length of stimulations for DMA scans ($n = 295$ events). Stimulus lengths ranged from 5 to 75 s; most frequent length (mode) was 35 s. **(C)** Average pain rating across all patients for all DMA scans for epochs of increases (left panel) and decreases (right panel) in ratings (time = 0 is start or end of the stimulus that induces pain), separated by sessions (session 1: prior to lidocaine treatment; session 2: post 6-hour treatment; and session 3: post 2-week treatment). The total amount of pain (spontaneous + Δ pain) decreased significantly with treatment. **(D)** Same as in **(C)** after subtracting spontaneous pain, which isolates touch-evoked DMA pain (Δ pain).

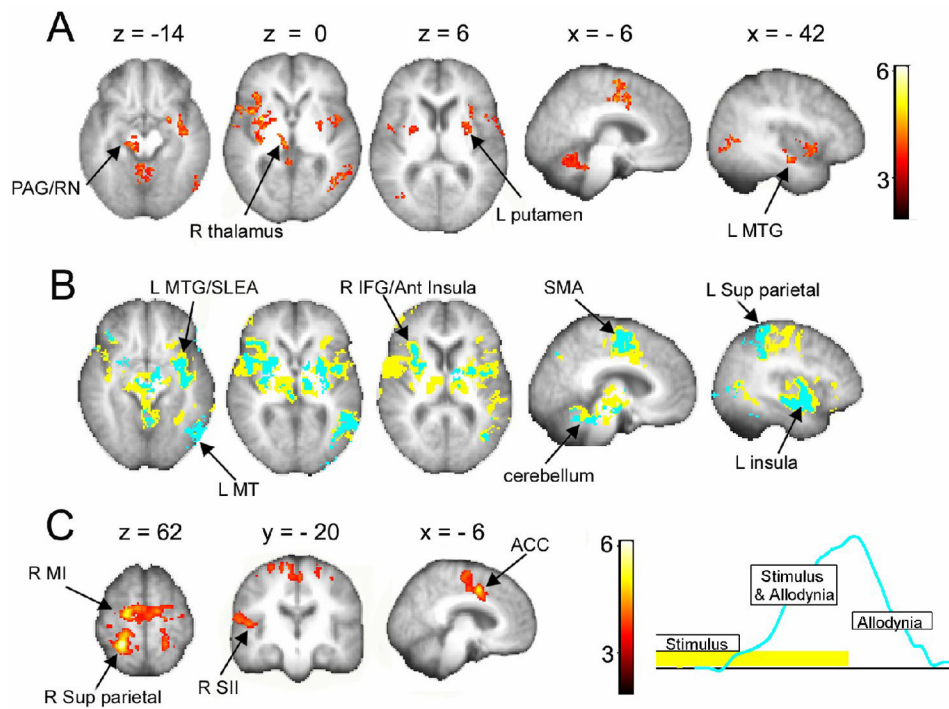


Figure 2. Brain activity for DMA in PHN patients

(A) Brain activity map for the comparison between DMA-evoking touch stimuli vs. non-painful touch stimuli, averaged across all treatment sessions. (B) Brain activity overlap between maps generated for DMA based on stimulus timings (yellow) and on ratings (blue). The map based on ratings is a subset of the map based on stimulus timings. (C) Results of contrasting the two maps in (B). Activity determined by stimulus timings is significantly larger in multiple brain regions than activity determined by rating of DMA. The opposite contrast does not yield any significant clusters. The right inset illustrates the time relationship between contrasted maps. Arrows indicate specific activated clusters. Both contrasts use spontaneous pain, pain duration and patient age as covariates of no interest. For abbreviations see Table 1. Activations are presented in standard space coordinates, shown in mm above the slices. Spatial orientation follows radiological convention with the left side of the brain shown on the right.

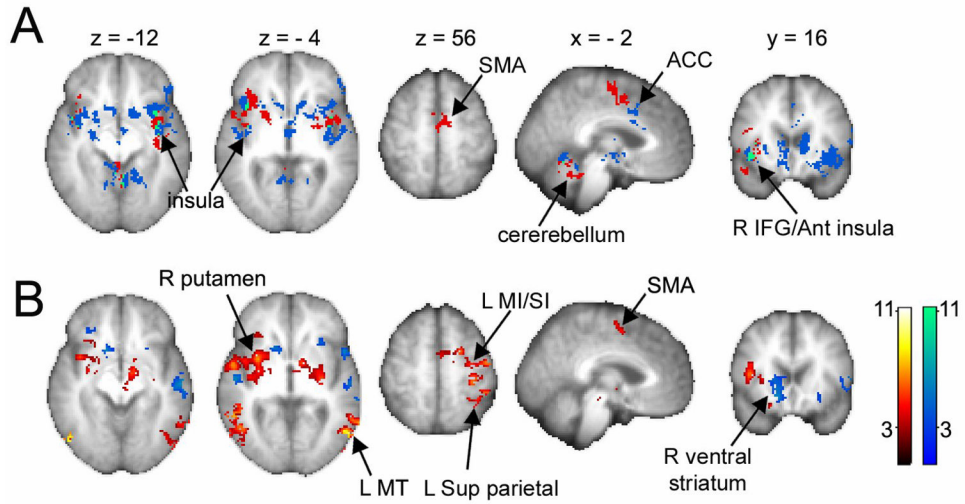


Figure 3. Comparison of brain regions activated for DMA and for spontaneous pain in PHN patients

(A) Brain activity map for DMA (red), spontaneous pain (blue, from [28]), and the conjunction of the two maps (green). Both activate similar brain regions but with minimal overlap (green). (B) Contrasting the two maps, after correcting for differences in perceived magnitude of total pain, shows differential representation for DMA (red) and spontaneous pain (blue) primarily, within different portions of the basal ganglia and insula; visual and sensorimotor (contralateral to the hand used in the ratings) regions are more prominently active in the DMA task. Arrows indicate specific activated clusters. For abbreviations see Table 1.

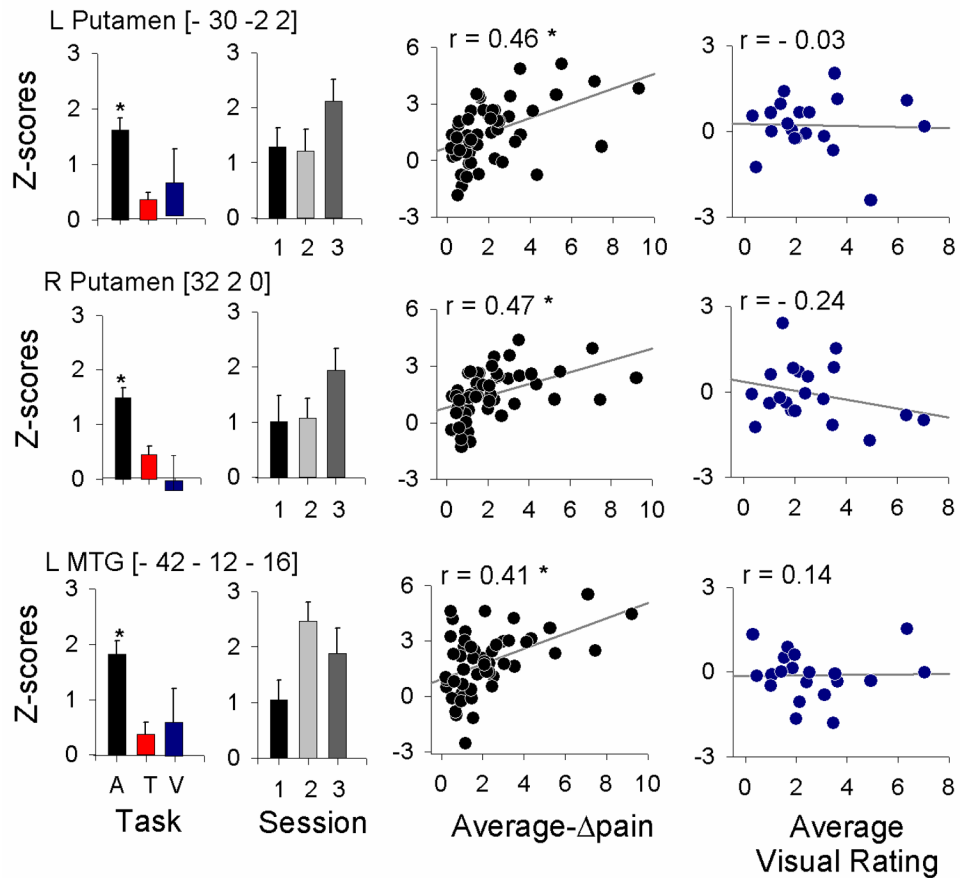


Figure 4. Average response properties for three brain regions that showed best specificity for DMA Left bar graphs indicate task dependence, where responses are shown during touch that induced DMA pain (A), non-painful touch (T), and visual bar ratings (V). All three areas show statistically significantly higher responses during DMA. Next bar graphs show responses during DMA at three treatment sessions (session 1: prior to Lidocaine treatment; 2: after a 6-hour treatment; and 3: after 2-week treatment). There were no significant treatment effects. Left scatter-grams indicate the relationship between DMA and regional activity, positively correlated in all three areas. Right scatter-grams show the relationship between visual ratings and brain activity. Asterisks indicate significance at $P < 0.01$; regression plots show 95% confidence interval.

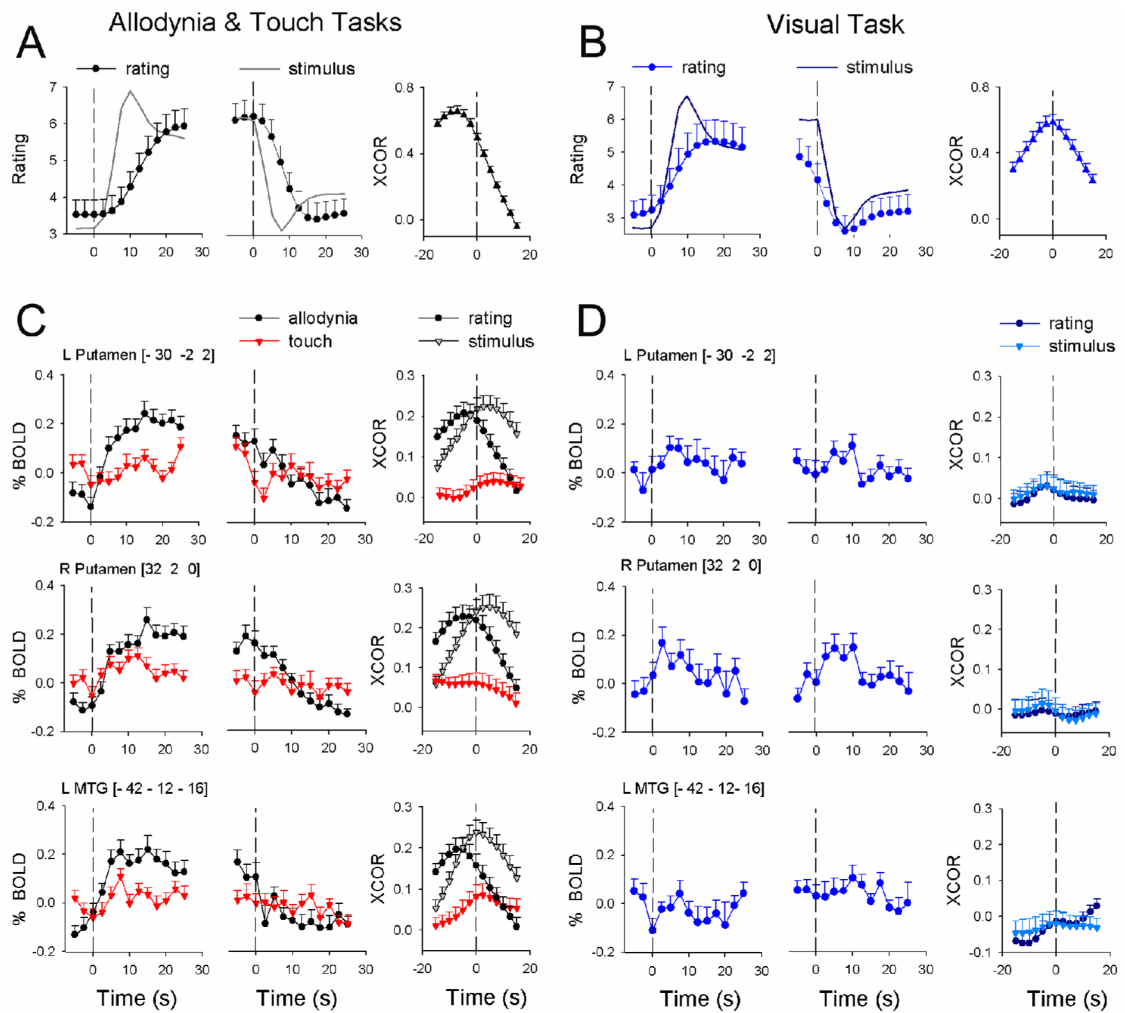


Figure 5. Temporal response properties for three brain regions that showed best specificity for DMA

A) shows stimulus (continuous line) and averaged ratings for DMA, relative to start and end of the stimulus (first and second panels, respectively). **B)** shows stimulus (continuous line) and averaged ratings for visual task (all convolved with hemodynamic response function). For both tasks, average cross-correlation (XCOR) between stimuli and ratings is also shown. **C)** The three rows show regional BOLD time courses relative to start and end of stimuli, as well as cross-correlations (XCOR) with stimuli and ratings, for DMA and non-painful touch. **D)** BOLD time courses and cross-correlations are shown for the visual task for the same brain regions as in **C)**.

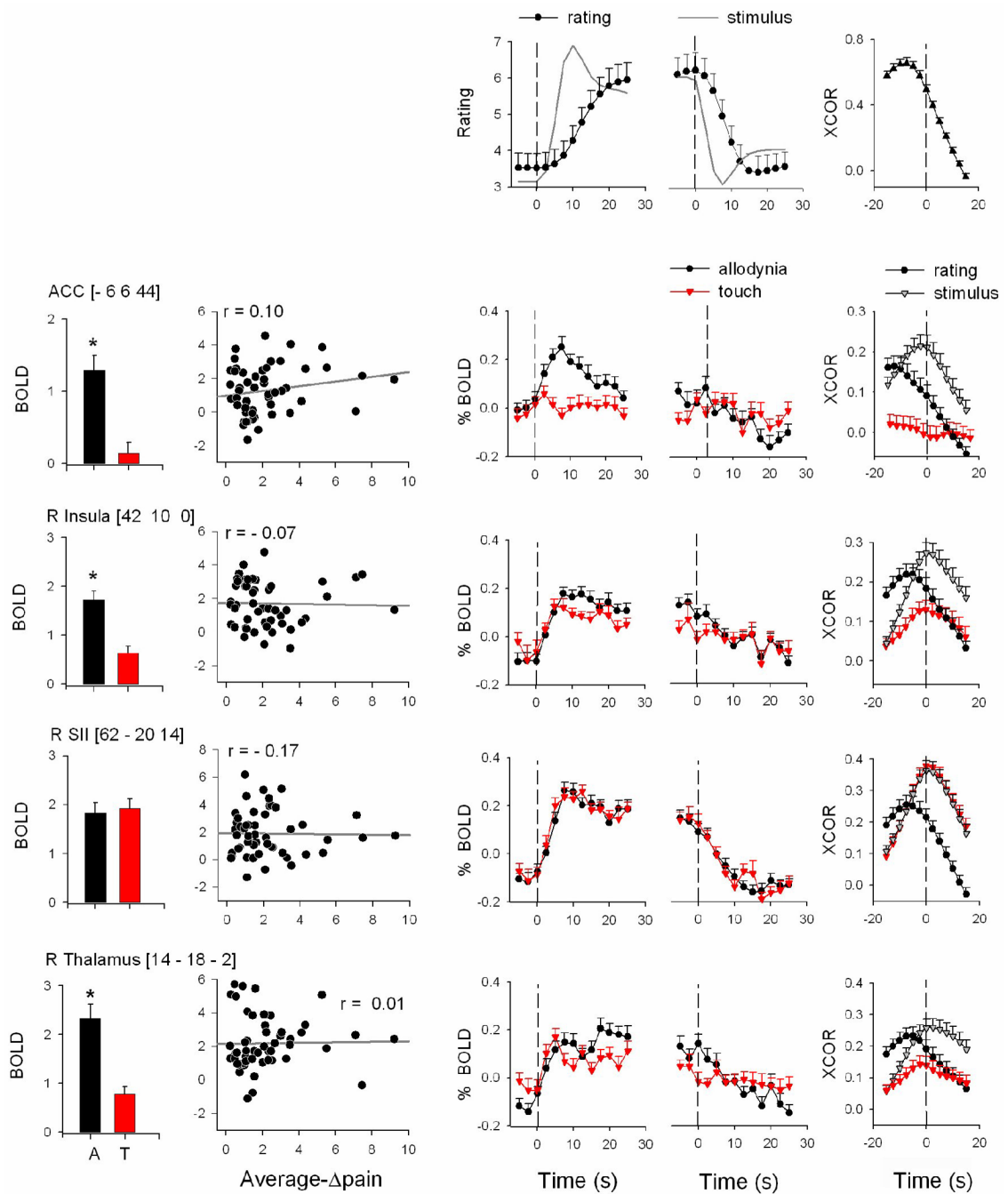


Figure 6. Response properties for four additional brain regions

Bar graphs indicate differential responses to DMA and touch tasks (A, T; black and red). Scatter-grams show the relationship between DMA ratings and activity. Time course of BOLD responses is also shown relative to start and end of stimuli (third and fourth panels from left). Cross-correlations (XCOR) among BOLD and stimuli and ratings are shown in right-most panels. Top row is the same as figure 5A.

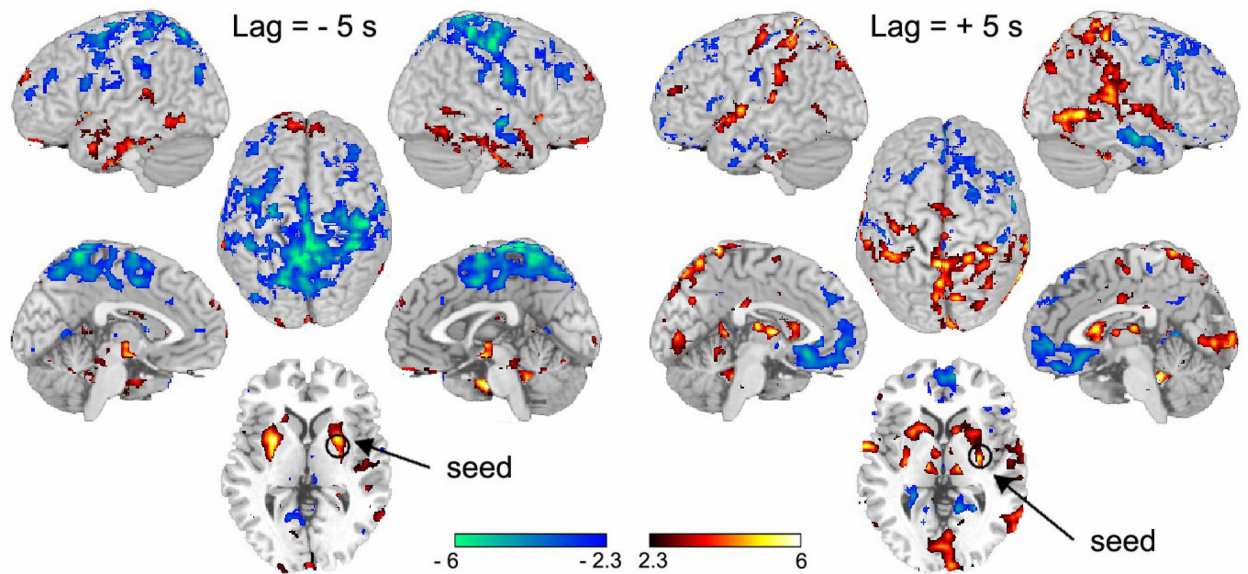


Figure 7. Evolution of brain connectivity in time for the signal best related to perception of DMA
 The time course of the left putamen was used as the seed, delayed by either -5 s (left) or by $+5$ s (right), and correlated to all brain voxels. Resultant maps show the brain network of regions correlated (red) and anti-correlated (blue) to the seed signal. In the left panel, large parts of the parietal cortex are anti-correlated, while brainstem, cerebellar, and inferior temporal areas are positively correlated with the delayed seed signal. In the right panel, thalamus and large parts of parietal cortex are correlated, while medial prefrontal cortex is anti-correlated with the delayed signal. For each map, left two images are lateral and medial views of right hemisphere; center top image is a dorsal view and bottom is a mid-horizontal slice at the level of the seed; right two images are lateral and medial views of left hemisphere.

Table 1

Brain regions activated for DMA

Region	Coordinates			Z-value	Index
	x	y	z		
L.MT (21/37)	-62	-60	-6	4.13	1
L.Insula	-40	10	-6	3.82	2
L.Amygdala/SLEA	-26	2	-16	3.85	2
L.MTG (21/35)	-42	-12	-16	3.76	2
L.Putamen	-30	-2	2	3.83	2
L.ACC (32)	-6	6	44	4.09	3
L.SMA (6)	6	2	56	5.05	3
R.Insula	42	10	0	4.64	4
R.Putamen	32	2	0	5.01	4
R.IFG/Ant Insula (47)	36	26	-8	4.68	5
R.Thalamus	14	-18	-2	4.47	5
R.SN/RN	8	-20	-12	3.40	5
R.PAG	6	-25	-8	2.90	5
Cerebellum	12	-62	-20	5.71	5

The contrast was done relative to stimulus timings, (*Sa - S_{tail}*), and contained 5 clusters: cluster 1, 461 voxels, $p < 10^{-3}$; cluster 2, 546 voxels, $p < 10^{-3}$; cluster 3, 556 voxels, $p < 10^{-3}$; cluster 4, 1332 voxels, $p < 10^{-8}$; cluster 5, 1338, $p < 10^{-8}$. *Abbreviations used:* L, left; R, right; Ant, anterior; ACC, anterior cingulate cortex; IFG, inferior frontal gyrus; MT, mid temporal (*visual motion*), MTG, medial temporal gyrus; OFC, orbitofrontal cortex; PAG, periaqueductal gray; RN, red nucleus; SMA, supplementary motor cortex; SLEA, sub-lenticular extended amygdala SN, substantia nigra. Numbers in parentheses = Brodmann areas.

Table 2

Brain areas activated for stimulus vs. DMA ratings

Region	Coordinates			Z-value		Index
	x	y	z			
R SII (2/40)	62	-20	14	3.25	1	
Sup Parietal Lobule (S/7)	24	-44	62	5.99	2	
R MI (4)	20	-14	66	4.92	2	
ACC (24/32)	-6	2	46	4.54	2	
L SMA (6)	-10	-10	68	4.49	2	
R SMA (6)	6	0	54	4.39	2	
SI (1/2)	22	-32	66	3.62	2	

The contrast was a fixed effects comparison of $((Sa - St) - (Ra - Rr)) / all$ and contained two clusters: cluster 1, 818 voxels, $p < 10^{-4}$; cluster 2, 4013 voxels, $p < 10^{-15}$. Abbreviations used: L, left; R, right; ACC, anterior cingulate cortex; MI, primary motor cortex; SII, primary somatosensory cortex; SI, secondary somatosensory cortex; SMA, supplementary motor cortex; Sup, superior. Numbers in parentheses = Brodmann areas.

Table 3

Contrasting BOLD signal between DMA and touch

	BOLD (rating is increasing)			BOLD (rating is decreasing)		
	Group	Time	Group × Time	Group	Time	Group × Time
L Putamen	14.7 (<10 ⁻⁵)	8.5 (<10 ⁻⁵)	5.0 (<10 ⁻⁵)	0.2 (0.7)	7.3 (<10 ⁻⁵)	3.6 (<10 ⁻⁴)
R Putamen	5.1 (0.03)	8.2 (<10 ⁻⁵)	3.2 (<10 ⁻⁵)	0.17 (0.7)	5.6 (<10 ⁻⁵)	3.4 (<10 ⁻⁴)
R Insula	4.2 (0.04)	14.2 (<10 ⁻⁵)	1.3 (0.2)	1.5 (0.2)	6.9 (<10 ⁻⁵)	1.2 (0.3)
ACC	27.5 (<10 ⁻⁵)	4.5 (<10 ⁻⁵)	4.6 (<10 ⁻⁵)	0.4 (0.5)	2.4 (<0.01)	1.9 (0.03)
L Amygdala/SLEA	10.3 (0.01)	7.7 (<10 ⁻⁵)	3.3 (<10 ⁻⁴)	0.03 (0.9)	3.5 (<10 ⁻⁴)	1.8 (0.05)
R SII	0.1 (0.8)	35.0 (<10 ⁻⁵)	0.6 (0.9)	0.01 (0.9)	29.2 (<10 ⁻⁴)	0.8 (0.6)
R Thalamus	0.1 (0.7)	12.3 (<10 ⁻⁴)	1.9 (0.03)	0.03 (0.9)	5.3 (<10 ⁻⁴)	1.5 (0.1)

Two-way ANOVA for time course of BOLD comparing: 1) between groups (pain and touch; F_{1, 95}), 2) across time (F_{12, 1140}), and 3) group by time interaction (F_{12, 1140}), shown separately for epochs where ratings are increasing or decreasing. *Abbreviations used:* L, left; R, right; ACC, anterior cingulate cortex; Ext, extended; SII, secondary somatosensory cortex. Numbers in red indicate significant outcomes.